Competing Relaxation Mechanisms in a Disclinated Nanowire: Temperature and Size Effects

K Zhou,[1] A. A. Nazarov,[2] and M. S. Wu[1,*]

[1]School of Mechanical and Aerospace Engineering, Nanyang Technological University, Singapore 639798
[2]Institute of Physics of Advanced Materials, Ufa State Aviation Technical University, 12 Karl Marx Street, 450000 Ufa, Russia

(Received 29 May 2006; published 16 January 2007)

This Letter reports a molecular dynamics study of the temperature and size dependence of disclination relaxation in a bicrystalline titanium nanowire. The simulations show that an unstable disclination may relax via crack nucleation and/or structural transformation. The critical disclination strength to nucleate a crack decreases with the nanowire diameter at 0 K, but an inverse relation may exist at higher temperatures. Similar relaxation mechanisms are operative in other hcp materials. The results suggest that grain boundaries in nanostructured materials can be disordered through disclinations which relax via amorphization.

DOI: 10.1103/PhysRevLett.98.035501 PACS numbers: 61.72.Lk, 62.25.+g

Disclinations are rotational linear defects, and along with dislocations, their translational analogues, were first introduced in continuum elasticity theory [1]. Both defects can be created in a hollow cylinder by cutting along a radial plane and displacing the cut faces relatively either by translation to a Burgers vector $\vec{b}$ to obtain a dislocation or rotation to a Frank vector $\vec{\omega}$ to obtain a disclination [1–3]. If $\vec{\omega}$ is parallel (or perpendicular) to the cylinder axis, the disclination is wedge (or twist) in character. The norm $\omega = |\vec{\omega}|$ is the disclination strength. The disclination is considered negative (or positive) if material needs to be filled in to close any gap due to the relative displacement (or taken away if the faces interpenetrate). Figure 1 shows an example of a negative wedge disclination in a Ti cylinder with the $[1\bar{1}00]$ tilt axis (for more details, see below).

The disclination concept is widely used to describe the structures and mechanical properties of nanoparticles, nanofilms, and bulk nanostructured materials [4–12]. Disclinations are observed in thin films grown on substrates [10] and in pentagonal nanoparticles [11]. They can form in grain boundaries (GBs) and their junctions during the compaction of nanopowders to obtain nanostructured materials [9]. They can arise in triple junctions in plastically deformed polycrystalline materials due to dislocation accumulation in GBs [12]. Such disclinations play a key role in grain subdivision during deformation [12], and can be inherited by bulk nanostructured materials produced by severe plastic deformation [6–8]. Indeed, disclinations have been observed directly via electron microscopy in metals such as copper and titanium subjected to severe plastic deformation [13] and in nanostructured iron produced by high-energy ball milling [14].

Since disclinations induce stress concentrations near their cores as well as long-range stresses, they can strongly influence the properties of nanostructured materials. For instance, they contribute significantly to the work hardening of nanocrystals [15] and to their plastic deformation via a rotational mechanism [4] that can be observed during molecular dynamics simulations of nanocrystal deformation [16]. Junction disclinations can also significantly influence the propagation of intercrystalline cracks in nanocrystals [17]. Hence, disclination-mediated processes are quite common in nanostructured materials.

A disclination can relax in different ways, the most common being crack nucleation. Disclinated cracks have been studied via continuum elasticity [18–20]. In [19], amorphization of the disclination core was suggested as a relaxation mechanism that can retard crack nucleation. In our atomistic studies of disclinated Ni and Ti bicrystalline nanowires [21,22], disclinations can initiate cracks above some critical strength ω_c which decreases with the nano-

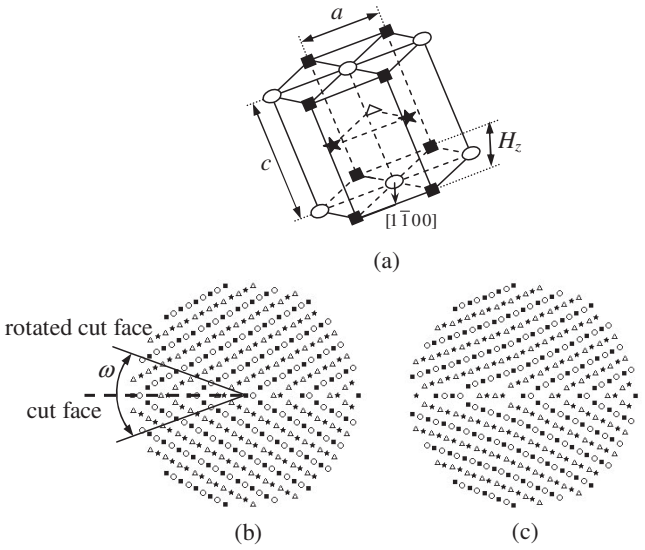

FIG. 1. Schematic view of (a) four layers of atoms over one period H_z along the $[1\bar{1}00]$ direction in an hcp lattice, (b) the $(1\bar{1}00)$ projection of a reference B bicrystal with a radial cut the faces of which are rotated relatively by ω, and (c) disclinated nanowire containing the reference B bicrystal on the right side and filled-in material on the left side.

wire diameter. Moreover, new grain nucleation at the crack tip can arrest crack growth in Ti [22]. The atomistic studies were carried out at zero temperature, although the relaxation mechanisms may be size and temperature dependent. As these mechanisms play a key role in the structural stability and strength properties of nanowires, nanofilms, and bulk nanostructured materials, the temperature and size effects on the relaxation of disclinated nano-objects warrant detailed investigations.

In this Letter, we report molecular dynamics (MD) simulations of disclinated Ti nanowires with diameters $D = 10$–20 nm at the temperatures $T = 0$, 298, and 600 K. We construct bicrystalline nanowires containing the $(11\bar{2}6)$ and $(11\bar{2}8)$ symmetrical tilt GBs, termed (B) and (AB) GBs, respectively, both with their $[1\bar{1}00]$ tilt axis parallel to the nanowire axis. The nanowires are infinitely periodic along the tilt axis. Figure 1(a) shows the $(1\bar{1}00)$ projection of four consecutive layers of atoms over one period H_z of the hexagonal close-packed (hcp) lattice. Negative wedge disclinations are inserted into reference bicrystals containing (B) or (AB) as GBs [22], see Figs. 1(b) and 1(c). The (B) boundary is a short period, special GB consisting of one type of structural units, while the (AB) boundary consists of two types of structural units [23]. Periodic boundary conditions are applied along the $[1\bar{1}00]$ direction, consistent with the plane strain condition [3]. MD relaxations of these systems are performed using the MATERIALS EXPLORER code [24], in which the modified embedded atom method (MEAM) potential is used to describe the atomic interactions [25]. The systems are equilibrated over the time intervals of 3 to 10 ps depending on D and ω.

The results show that for each D and T there exists a critical disclination strength $\omega = \omega_c$ above which a crack initiates from the disclination core. When ω approaches ω_c from below, however, structural transformation may precede or follow the crack nucleation, depending on D and T. The type of structural transformation depends on the GB structure.

The ω_c versus D simulation results for nanowires containing the (B) GB are presented in Fig. 2. At $T = 0$ K, ω_c monotonically decreases with D according to $\omega_c \propto D^{-0.78}$, no structural transformation precedes crack formation, and the growing crack can be arrested by the nucleation of a new hexagonal close-packed grain whose [0001] axis lies parallel to the tilt axis [22]. However, at $T = 298$ and 600 K the dependencies of ω_c on D are similar but are quite different from that at $T = 0$ K (Fig. 2). This indicates common stress release mechanisms at these temperatures, different from that at $T = 0$ K. For $T = 298$ and 600 K and $10\ \text{nm} \leq D \leq 14$ nm, little structural transformation is observed before crack nucleation, and ω_c in this diameter range is significantly lower than that at $T = 0$ K. This initial reduction of ω_c with T can be explained by the nucleation of a thermally activated crack at nonzero temperatures. This behavior is consistent with a statistical analysis provided in [26], which shows that the failure stress due to a thermally activated microcrack at temperatures higher than a certain limit does not depend on T and can be twice less than that at $T = 0$ K.

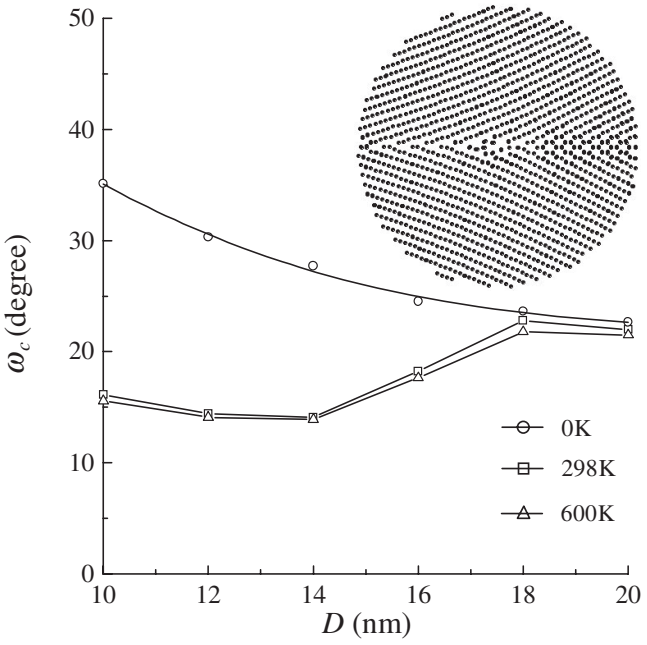

FIG. 2. The D- and T- dependence of ω_c for crack nucleation in a bicrystalline Ti nanowire containing the $(11\bar{2}6)$ tilt boundary. The atom configuration in the central region (8 nm diameter) of a 20 nm diameter nanowire is shown for $T = 298$ K and $\omega = 20.6° < \omega_c$. A new grain appears as a thin band (previously the GB) on the right side of the nanowire.

Figure 2 also shows that ω_c first decreases with D at all the temperatures. This reflects an increase of stress concentration at the disclination core with D. However, ω_c increases with D in the range $14\ \text{nm} \leq D \leq 18$ nm at $T = 298$ and 600 K. Examination of the simulated structures shows that at these finite temperatures an increase of ω results first in the transformation of a part of the GB into a new grain, see Fig. 2. For $\omega \geq \omega_c$ this new grain formation is followed by crack nucleation. The larger the diameter, the higher is the tendency to form a new grain. Apparently, the new grain formation is an alternative stress release mechanism that retards the crack formation and results in an increase of ω_c with D. For $D > 18$ nm, the disclination stress becomes dominating and ω_c starts to decrease with D again as in the case of $T = 0$ K. Thermal activation appears to play a less significant role at large D.

The dependencies of ω_c on D for disclinations inserted into the AB bicrystal are shown in Fig. 3. The curves are similar to those for the B bicrystal, suggesting a similar operation of instabilities competitive with crack nucleation. However, in the range $D > 14$ nm at the finite temperatures an increasingly disordered region near the disclination core, rather than new grain nucleation, is

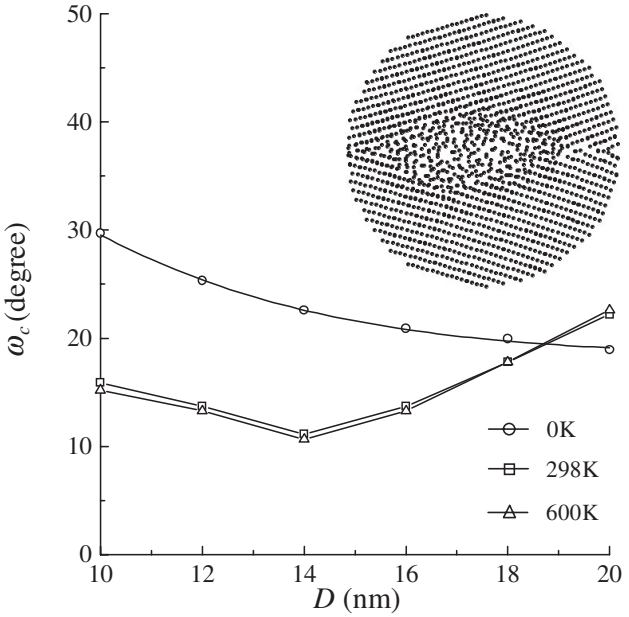

FIG. 3. The D- and T- dependence of ω_c for crack nucleation in a bicrystalline Ti nanowire containing the $(11\bar{2}8)$ tilt boundary. The atom configuration in the central region (8 nm diameter) of a 20 nm diameter nanowire is shown for $T = 600$ K and $\omega = 18.9° < \omega_c$.

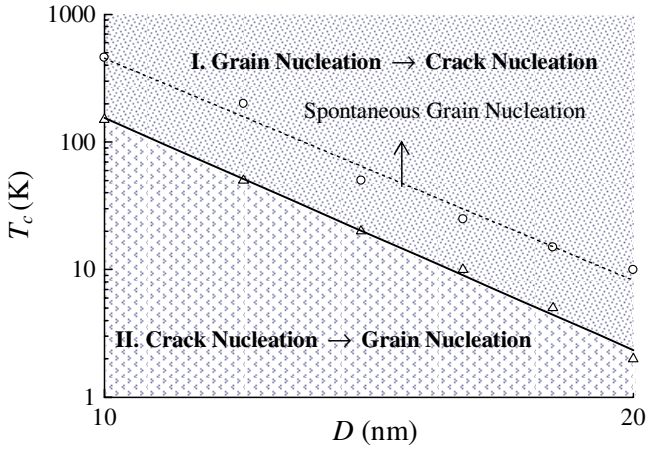

FIG. 4 (color online). Relaxation mechanism map of nanowires containing $(11\bar{2}6)$ tilt boundaries. The regions above and below the solid line indicate domains with different sequences of operating mechanisms. Above the dashed line spontaneous grain nucleation occurs.

observed as ω increases. As assumed in [19], amorphization or, more generally, disorder of the disclination core, retards the crack nucleation. Here we observe this disorder directly via MD simulations, see Fig. 3. The size of the disordered region increases with D, and the disordering of the core is followed by crack nucleation when $\omega \geq \omega_c$. As seen in Fig. 3, the disordering results in an increase of ω_c with D beyond 14 nm. Indeed, ω_c at the finite temperatures can be larger than that at 0 K, as is the case at $D = 20$ nm.

The above simulations reveal that ω_c is strongly size and temperature dependent. The inverse ω_c versus D relation may limit grain size refinement in nanostructured materials, as is the case with the inverse Hall-Petch relation for the yield strength of nanostructured materials and multilayered nanocomposites [27,28]. Also, a higher T encourages structural transformation (raising ω_c) while it also promotes thermal activation of cracks (lowering ω_c). This is coupled to the size effect because smaller sizes limit the structural transformation.

The results obtained for nanowires containing the B bicrystal are summarized in Fig. 4 by a mechanism map plotting critical temperature T_c against nanowire diameter D in logarithmic scale. In region I above the solid straight line new grain nucleation always occurs before crack nucleation at ω_c, while in region II below the solid line crack nucleation occurs before grain nucleation. Structural transformations at crack tips have been revealed by MD simulations: bcc to fcc transformation in nanocrystalline Fe [29] and martensitic transformations in Fe-Ni and Ti-V alloys [30]. However, to the authors' knowledge no structural transformations preceding crack formation have been predicted. Above the dashed line in Fig. 4, new grain nucleation can occur in the bicrystal in the absence of a disclination. This recrystallization behavior is specific for the (B) GB and is not observed for the (AB) GB. A simple analysis shows that this is caused by a small mismatch between the periods of the bicrystal and the emerging grain for the former case and a large mismatch for the latter.

Figure 4 also provides a global perspective of the coupled size and temperature effect. In particular, $\log(T_c)$ decreases linearly with $\log(D)$ for the transition in the operating sequence of relaxation mechanisms and in the spontaneous grain nucleation. At and above the room temperature crack nucleation is always preceded by grain nucleation for all the diameters considered. Moreover, in the region between the solid and dashed lines new grain nucleation can occur only in the presence of a disclination and it will be followed by crack nucleation if the disclination strength is critical.

Further calculations have been carried out for disclinated $[1\bar{1}00]$ bicrystals of other hcp metals with (B) and (AB) as reference GBs. For 16 hcp metals whose MEAM potentials are given in [25], crack nucleation can be found in all of them, amorphization in 7 of the metals (e.g., titanium, yttrium, and ruthenium) and grain nucleation in several metals such as hafnium. Figure 5 illustrates crack nucleation in cobalt and amorphization in yttrium. These relaxation mechanisms also depend on temperature and size in addition to the material type, the GB character, and the disclination strength.

The present results show that crack nucleation is in general a favorable channel of relaxation. As for structural transformation, new grain nucleation tends to occur in cases when the GB period of the bicrystal and the lattice period of the new grain are similar, whereas disorder of the

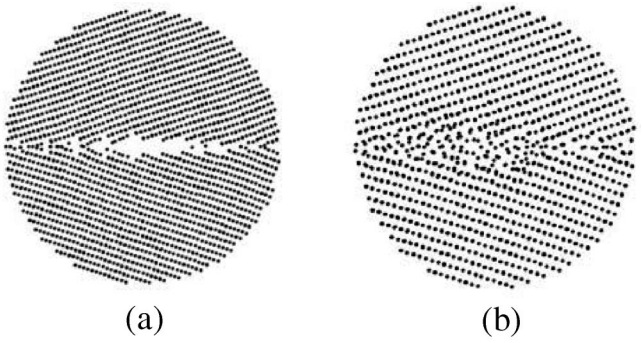

FIG. 5. Modes of relaxation in the central 8 nm diameter region of a 20 nm diameter nanowire with the $(11\bar{2}8)$ reference boundary at $T = 600$ K: (a) nanocrack in cobalt at $\omega = 13°$, and (b) amorphization in yttrium at $\omega = 11.9°$.

disclination core seems to be more general and will likely occur in cases when a disclination is inserted into a bicrystal (or into junctions of GBs in polycrystals) with general GBs. The disorder phenomenon, previously predicted by phenomenological calculations, is directly observed in our MD simulations.

The prediction of disorder may have an implication for the problem of boundary structures in bicrystals and nanostructured materials, which has long been debated. Based on MD simulations, Keblinski *et al.* [31,32] found that general GBs have the same amorphous structures in both bicrystals and nanocrystals. However, general GBs in bicrystals can have an ordered structure [33]. The present results can be an important indication of the difference between equilibrium GB structures in bicrystals or well annealed polycrystals and nonequilibrium GBs containing extrinsic defects, i.e., defects with long-range stresses in nonequilibrium GBs can result in disordering of the atomic structure. Consequently, the amorphous character of GBs in nanocrystals may arise from the presence of extrinsic defects such as disclinations.

The authors acknowledge the financial support of the Agency for Science, Technology and Research, Singapore (Grant No. 0321010019) in this investigation. A. A. Nazarov also acknowledges a partial support of his research by the Russian Science Support Foundation.

*Corresponding author.
Email address: mmswu@ntu.edu.sg

[1] V. Volterra, Ann. Éc. Normale Sup., Paris **24**, 401 (1907).
[2] R. de Wit, J. Res. Natl. Bur. Stand., Sect. A **77**, 49 (1973); **77**, 359 (1973); **77**, 607 (1973).
[3] A. E. Romanov and V. I. Vladimirov, in *Dislocations in Solids*, edited by F. R. N. Nabarro (North-Holland, Amsterdam, 1992), Vol. 9, p. 191.
[4] I. A. Ovid'ko, Science **295**, 2386 (2002).
[5] M. Yu. Gutkin and I. A. Ovid'ko, Rev. Adv. Mater. Sci. **4**, 79 (2003).
[6] A. A. Nazarov, A. E. Romanov, and R. Z. Valiev, Acta Metall. Mater. **41**, 1033 (1993).
[7] A. A. Nazarov, A. E. Romanov, and R. Z. Valiev, Scr. Mater. **34**, 729 (1996).
[8] R. Z. Valiev, R. K. Islamgaliev, and I. V. Alexandrov, Prog. Mater. Sci. **45**, 103 (2000).
[9] V. G. Gryaznov and L. I. Trusov, Prog. Mater. Sci. **37**, 289 (1993).
[10] X. Jiang and C. L. Jia, Appl. Phys. Lett. **69**, 3902 (1996).
[11] M. J. Yacamán, J. A. Ascencio, H. B. Liu, and J. Gardea-Torresdey, J. Vac. Sci. Technol. B **19**, 1091 (2001).
[12] V. V. Rybin, *Large Plastic Deformations and Fracture of Metals* (Metallurgiya, Moscow, 1986) (in Russian).
[13] M. Motylenko, V. Klemm, P. Klimanek, T. Pavlovitch, and H. Straube, J. Alloys Compd. **378**, 93 (2004).
[14] M. Murayama, J. M. Howe, H. Hidaka, and S. Takaki, Science **295**, 2433 (2002).
[15] V. G. Gryaznov, M. Yu. Gutkin, A. E. Romanov, and L. I. Trusov, J. Mater. Sci. **28**, 4359 (1993).
[16] T. Shimokawa, A. Nakatani, and H. Kitagawa, Phys. Rev. B **71**, 224110 (2005).
[17] V. A. Pozdnyakov and A. M. Glezer, Phys. Solid State **47**, 817 (2005).
[18] V. V. Rybin and I. M. Zhukovskii, Sov. Phys. Solid State **20**, 1056 (1978).
[19] M. Yu. Gutkin and I. A. Ovid'ko, Philos. Mag. A **70**, 561 (1994).
[20] M. S. Wu and H. Zhou, Int. J. Fract. **82**, 381 (1996).
[21] K. Zhou, A. A. Nazarov, and M. S. Wu, Phys. Rev. B **73**, 045410 (2006).
[22] M. S. Wu, K. Zhou, and A. A. Nazarov, Model. Simul. Mater. Sci. Eng. **14**, 647 (2006).
[23] D. Farkas, Metall. Mater. Trans. A **25A**, 1337 (1994).
[24] Information about Materials Explorer is available through http://www.cachesoftware.com/materialsexplorer/
[25] M. I. Baskes and R. A. Johnson, Model. Simul. Mater. Sci. Eng. **2**, 147 (1994).
[26] Robin L. Blumberg Selinger, Z. G. Wang, W. M. Gelbart, and A. Ben-Shaul, Phys. Rev. A **43**, 4396 (1991).
[27] M. A. Meyers, A. Mishra, and D. J. Benson, Prog. Mater. Sci. **51**, 427 (2006).
[28] A. Misra, J. P. Hirth, and H. Kung, Philos. Mag. A **82**, 2935 (2002).
[29] A. Latapie and D. Farkas, Phys. Rev. B **69**, 134110 (2004).
[30] P. Dang and M. Grujicic, Acta Mater. **45**, 75 (1997).
[31] P. Keblinski, S. R. Phillpot, D. Wolf, and H. Gleiter, Phys. Rev. Lett. **77**, 2965 (1996); J. Am. Ceram. Soc. **80**, 717 (1997).
[32] P. Keblinski, D. Wolf, S. R. Phillpot, and H. Gleiter, Scr. Mater. **41**, 631 (1999).
[33] S. von Alfthan, P. D. Haynes, K. Kaski, and A. P. Sutton, Phys. Rev. Lett. **96**, 055505 (2006).